Chemical and Process Engineering Research
ISSN 2224-7467 (Paper) ISSN 2225-0913 (Online)
Vol.20, 2014
www.iiste.org

Stability of Some Copper Ternary Alloys in Chloride Solutions Polluted by Sulfide Ions

Hashem M. Nady[1], Mohammed M. El-Rabiei[1] and Waheed A. Badawy*[2]
1 Chemistry Department, Faculty of Science, Fayoum University, Fayoum-Egypt
2 Chemistry Department, Faculty of Science, Cairo University, 12 613 Giza- Egypt
*Email of the corresponding author: wbadawy@cu.edu.eg, wbadawy50@hotmail.com

Abstract
The electrochemical performance of three copper alloys was investigated in simulated marine solution polluted by sulfide ions. Polarization techniques and electrochemical impedance spectroscopy, EIS, were used. Surface examination and morphological studies were employed. The results showed that the Cu-10Ni-10Zn alloy is more stable than the other two alloys. The alloy surface was covered by a barrier layer protecting it from corrosion. The thickness and resistance of the barrier layer formed on the Cu-10Ni-10Zn alloy increases with the increase of the immersion time. The mechanism of the corrosion process and the barrier film formation was discussed. A comparison was made between the electrochemical stability of the three alloys in sulfide polluted chloride solution. The incorporation of Ni in the Cu_2O barrier film leads to its stabilization and the stability is enhanced by the presence of Zn. The results leads to the recommendation of the Cu-10Ni-10Zn alloy for applications in sulfide polluted marine environments.
Keywords: Copper alloys, EIS, Polarization, SEM, Passive Films.

1. Introduction

The physical properties of copper-based alloys are very attractive and lead to their application in a several technologically important industries. The high corrosion resistance and reasonable price have led to their use as materials for condensers and heat-exchange tubes in power-generation industry, especially whenever marine water is used [1, 2]. The corrosion behavior depends essentially on the barrier film formed on the alloy surface. Most of the barrier films formed on metals and alloys are suffering from accelerated corrosion when exposed to seawater because of the aggressiveness of the chloride ions. It is well known that the dezincification of Cu-Zn alloys in the presence of chloride ions is more pronounced in the zinc-rich phase. Al is commonly used in condenser tubes to decrease the rate of the dezincification process and a ratio up to 2 wt. % of Al was found to be necessary. The presence of aluminum increases the corrosion resistance of the alloy, especially in neutral solutions; it provides good wear properties and resistance to high temperature oxidation [3, 4]. The structure of the barrier film formed on Ni containing Cu alloys in simulated seawater was found to consist of two layers. An outer CuO layer with chemisorbed water molecules and traces of chloride ions, and an inner Cu_2O layer containing Ni^{2+} and Ni^{3+} [5-7]. The good corrosion resistance of the Cu-Al-Ni alloys in neutral solutions is due to the presence of a more stable protective layer of alumina, which builds up quickly on the surface post-exposure to the corrosive environment and the passivation process is based on the fact that aluminum has a greater affinity towards oxygen than copper and a considerable stability of Al_2O_3 than Cu_2O in neutral solutions [8-10]. The essential role of Ni in the passivation of Cu-Ni alloys was attributed to its incorporation into the Cu (I) oxide which is formed as corrosion product [11]. The incorporation of nickel ions reduces the number of cation vacancies that normally exist in Cu (I) oxide [12]. In marine solutions, copper and its alloys are facing service corrosion problems due to sulfide pollution, which is present in the form of hydrosulfide (HS^-) ions in nearly neutral media. These ions are known to promote the corrosion of copper and its alloys [13-15]. Sulfide pollution of seawater at the coastal areas can occur from industrial waste discharge, biological and bacteriological processes in seawater (seaweed, marine organisms or microorganisms, sulfide reducing bacteria). It has been reported that the corrosion rate of copper alloys increases by a factor of 10-30 times in sulfide polluted seawater [16]. The aggressiveness of sulfide ions, especially, in chloride solutions to attack metallic constructions, especially those containing Cu makes the investigation of the electrochemical behavior of Cu-ternary alloys like Cu-10Al-10Zn, Cu-10Al-10Ni and Cu-10Ni-10Zn an important subject worthy of intensive investigations.

The objective of this paper is to evaluate the corrosion rate and corrosion resistance of some copper ternary alloys in 3.5% NaCl polluted by sulfide ions. The mechanism of corrosion processes taking place at the electrode/solution interface will be discussed, and a categorization of the three investigated alloys according their stability in this aggressive medium can be made. The recommendation of the best material for industrial applications in sulfide polluted marine water is a main task.

2. Experimental details

The working electrodes were made from commercial grade Cu-Al-Zn, Cu-Al-Ni and Cu-Ni-Zn rods, mounted into appropriate glass tubes by two-component epoxy resin leaving a surface area of 0.2 cm^2 to contact the solution. The mass spectrometric analysis of the electrodes used is presented in Table 1.

Table 1: Mass spectrometric analysis for the different electrode materials in mass%.

Sample	Cu	Al	Ni	Zn	Mn	Sn	Fe	Si	Mg
Cu-10Al-10Zn	79.14	10.40	0.00	10.20	0.01	0.02	0.21	0.01	0.01
Cu-10Al-10Ni	76.00	11.28	9.95	0.10	0.02	0.14	2.26	0.24	0.01
Cu-10Ni-10Zn	81.31	0.60	8.07	9.71	0.01	0.02	0.06	0.22	0.00

The electrochemical cell was a three-electrode all-glass cell, with a platinum counter electrode and saturated calomel, SCE, reference electrode. Before each experiment, the working electrode was abraded using successive grades of emery papers down to 2000 grit. The electrode was washed thoroughly with distilled water, and transferred quickly to the cell. The electrochemical measurements were carried out in a stagnant, naturally aerated 3.5 (mass, m/volume, v) % NaCl containing 2 ppm S^{2-} solution. The polarization experiments and electrochemical impedance spectroscopic investigations were performed using a Voltalab PGZ 100 "All-in-one" Potentiostat/Galvanostat. The potentials were measured against and referred to a saturated calomel reference electrode, SCE, (0.245 V vs. the standard hydrogen electrode, SHE). The polarization experiments were carried out at a scan rate of 5 mV s^{-1} and the cyclic voltammetry measurements were carried out using a scan rate of 10 mV s^{-1} in the potential range -800 to 500 mV. The total impedance, Z, and phase shift, θ, were measured in the frequency range from 0.1 to 10^5 Hz. The superimposed ac-signal amplitude was 10 mV peak to peak. Each experiment was carried out at least twice. Details of experimental procedures were as described elsewhere [10, 17].

3. Results and discussion

3.1. Cyclic polarization measurements

The cyclic voltammograms for the Cu-alloys under investigation were recorded in a stagnant naturally aerated neutral 3.5 (m/v) % NaCl containing 2 ppm sulfide solution at a scan rate of 10 mV s^{-1} and 25 ^oC. The concentration of sulfide ion was always controlled and readjusted each 15 min, since it is well known that the half-life time of sulfide ion of initial concentration of about 4 ppm in air saturated seawater is about 20 min [18]. Fig. 1 presents the results of potential cycling in the potential range -800 to +500 mV. For comparison the CV of pure Cu was recorded under the same conditions and presented as inset in Fig.1. For Ni containing alloys, Cu-10Al-10Ni and Cu-10Ni-10Zn the CV curve is characterized by a single anodic peak and one cathodic peak, whereas the Cu-10Al-10Zn shows a clear anodic peak and a small shoulder, like that obtained with copper. Generally, cyclic voltammograms for copper and many copper alloys often show two anodic peaks in chloride containing solutions (cf. Fig. 1 inset), the first is related to the formation of CuCl film on the metal surface. The breakdown of this film by the complexation-dissolution and copper oxidation results in the second peak. The presence of only one anodic peak for the alloys can be explained on the basis of formation of aluminum and/or zinc hydroxide/oxide layer along with the CuCl surface layer, which prevents its breakdown [19, 20]. The aluminum and/or zinc hydroxide layer prevents the direct copper-chloride reaction on the surface, and so only one anodic peak could be recorded. For Cu-alloys containing Ni the dissolution of copper is inhibited, especially in the presence of Zn, and so a large cathodic peak represents electro-reduction of the soluble copper species [21]. The cyclic voltammograms of the alloys in chloride solutions containing sulfide ions have the same general shape like those recorded in chloride solutions free from sulfide ions, which means that the mechanism of the corrosion process does not change. In the presence of sulfide ions the anodic peak height increases which emphasizes an increase in the corrosion rate.

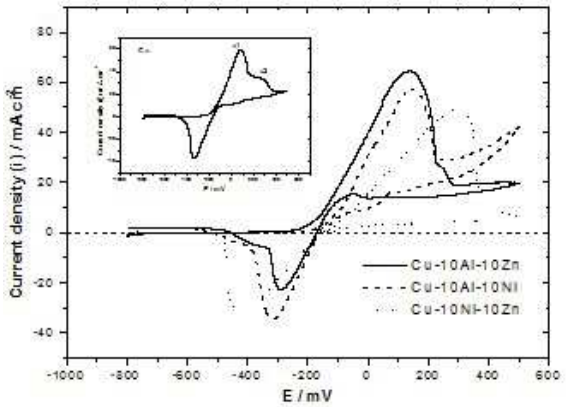

Fig.1: Cyclic voltammograms of Cu-10Al-10Ni, Cu-10Al-10Zn and Cu-10Ni-10Zn alloys in a stagnant naturally aerated neutral 3.5 % NaCl containing 2 ppm S^{2-} solution at 25 ˚C and scan rate of 10 mVs^{-1}.
Fig.1: (inset) Cyclic voltammograms of Cu in a stagnant naturally aerated neutral 3.5 % NaCl containing 2 ppm S^{2-} solution at 25 ˚C and scan rate of 10 mVs^{-1}.

3.2. Potentiodynamic polarization measurements

The potentiodynamic polarization curves of the three alloys immersed in stagnant naturally aerated neutral 3.5% (m/v) NaCl solution polluted by sulfide ions are presented in Fig. 2. The characteristic parameters of the corrosion of the three alloys i.e. the corrosion potential, E_{corr}, the corrosion current density, i_{corr}, the anodic, $ß_a$ and cathodic, $ß_c$, Tafel slopes and the rates of corrosion were calculated and presented in Table 2. The Tafel slopes were calculated from the linear anodic and cathodic branches of the Tafel lines. The corrosion current density and corrosion potential were extrapolated from the intersection of the Tafel lines. The i_{corr} was used for the calculation of the corrosion rate in mmy^{-1} according to the Faraday's law:

$$\text{Corrosion rate } (mmy^{-1}) = k \times i_{corr} (\mu A cm^{-2}) \times (M \text{ g mol}^{-1} / n \ / d \ (gcm^{-3})$$

The factor k includes the Faraday's constant, and the metric and time conversion factors, d is the density, M the molecular mass and n the number of equivalents (number of exchanged electrons in the corrosion process).

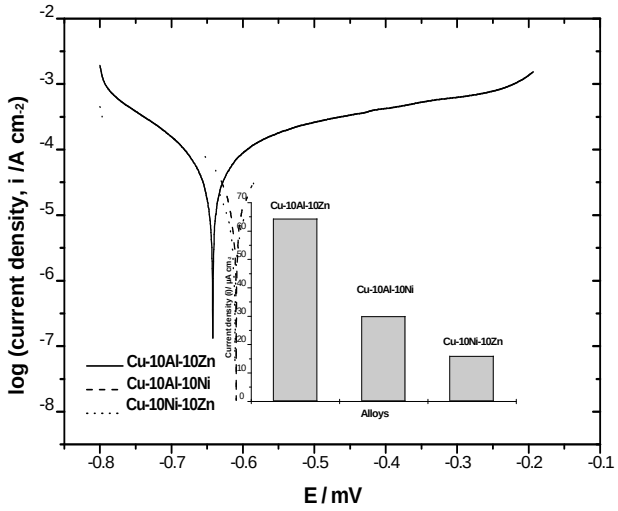

Fig. 2: Potentiodynamic polarization curves for Cu-10Al-10Ni (----), Cu-10Al-10Zn (___) and Cu-10Ni-10Zn (…..) alloys in a stagnant naturally aerated neutral 3.5 % NaCl containing 2 ppm S^{2-} solution at 25 ˚C and scan rate of 5 mVs^{-1}.
Fig. 2: (inset). The corrosion current density of the three different alloys after 240 h immersion in stagnant naturally aerated 3.5 % NaCl containing 2 ppm S^{2-} solution at 25 ˚C.

Table 2: Polarization parameters and rates of corrosion of the different Cu- alloys after 240 h of electrode immersion in stagnant naturally aerated neutral 3.5 % NaCl containing 2 ppm S^{--} at 25 ^{o}C.

Alloys	E_{corr} / mV	i_{corr} / µA cm^{-2}	$ß_a$ /mV	$ß_c$ /mV	Corr.Rate/µm y^{-1}
Cu-10Al-10Zn	-641	64	200	-139	760
Cu-10Al-10Ni	-609	30	146	-101	348
Cu-10Ni-10Zn	-610	16	219	-90	187

The presence of Ni in the Cu-alloy shifts its potential to more positive values, especially, in the presence of Zn. Also, the corrosion rate of the Cu-10Ni-10Zn alloy is less than one fourth of the Cu-10Al-10Zn alloy. Oxides of Ni, Zn and the corrosion products form a compact layer adherent to the alloy surface [22]. Comparison of the corrosion rate of the three investigated alloys in the polluted chloride solution, presented as corrosion current density, is shown as inset in Fig. 2. The effect of addition of sulfide ions to chloride solution on the corrosion behavior of the alloys is clearly presented on Fig. 3. It presents the potentiodynamic polarization curves of the alloy, namely Cu-10Al-10Zn, in chloride solutions free and containing sulfide ions. The potentiodynamic polarization curves of the other two alloys are similar. It is clear that the addition of sulfide ions to the chloride solution increases the corrosion current density; also, it shifts the corrosion potential to more negative values.

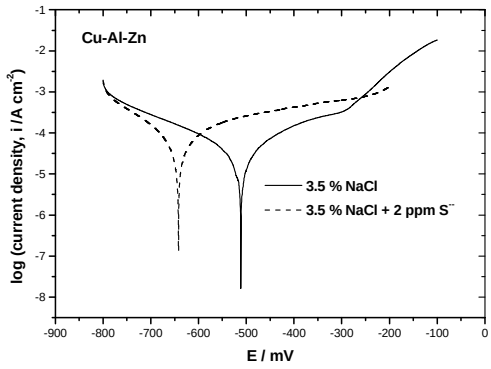

Fig.3: Potentiodynamic polarization curves for Cu-10Al-10Zn alloys in a stagnant naturally aerated neutral 3.5 % NaCl in absence (___) and presence (-----) of 2 ppm S^{2-} solution at 25 ◦C and scan rate of 5 mVs^{-1}.

For comparison, the characteristic parameters of the corrosion of the three alloys in chloride 3.5 (m/v) % NaCl solution free from sulfide ions are presented in Table 3.

Table 3: Polarization parameters and rates of corrosion of the different Cu- alloys after 240 h of electrode immersion in stagnant naturally aerated neutral 3.5 % NaCl at 25 oC.

Alloys	E_{corr}/mV	i_{corr} / µAcm^{-2}	$ß_a$ /mV	$ß_c$ /mV	Corr.Rate/µm y^{-1}
Cu-10Al-10Zn	-510	23.3	129	-144	274
Cu-10Al-10Ni	-464	7.4	122	-118	88
Cu-10Ni-10Zn	-442	0.8	77	-112	9

The accepted cathodic reaction occurring on Cu and Cu-based alloys in aqueous solutions is always represented by the oxygen reduction [7]:

$$O_2 + 2H2O + 4e^- \rightarrow 4OH^- \quad (1)$$

The anodic dissolution and film formation on Cu surface in chloride solutions can be represented by the reactions [7, 22, 23]:

$$Cu + 2Cl^- \rightarrow CuC_{l2}^- + e^- \quad (2)$$

It was suggested that the presence of $CuCl_2^-$ at the metal surface leads to hydrolysis reaction and the formation of Cu_2O [23] according to:

$$2CuCl_2^- + H_2O \rightarrow Cu_2O + 4Cl^- + 2H^+ \quad (3)$$

In Al containing alloys the surface dissolution of Al leads to an additional passivation process and formation of Al_2O_3 according to [23, 24]:

$$Al + 4\,Cl^- \rightarrow AlCl_{4-} + 3\,e^- \quad (4)$$

$$2\,AlCl_{4-} + 3\,H_2O \rightarrow Al_2O_3 + 6H^+ + 8\,Cl^- \quad (5)$$

Chloride ions are capable of destroying the Al_2O_3 layer at the first step, which allow Al to dissolve into the solution and hence higher corrosion rates were recorded.

$$Al^{3+}\ (\text{in } Al_2O_3.\,nH_2O \text{ crystal lattice}) + Cl^- \rightarrow Al(OH)_2Cl + 2H^+ \quad (6)$$

or

$$Al^{3+}(\ \text{in } Al_2O_3.\,nH_2O \text{ crystal lattice}) + 2Cl^- \rightarrow Al(OH)_2Cl_{2-} + 2H^+ \quad (7)$$

Progression of the above reactions causes the breakdown of the Al_2O_3 layer in some places. The formed hydroxyl aluminum chloride hydrolysis causes local acidity which increases the corrosion rate [24].

$$AlCl_{4-} + 2\,H_2O \rightarrow Al(OH)_2Cl_{2-} + 2H^+ + 2Cl^- \quad (8)$$

In the Zn containing alloys a passivation process involving the formation of Zn-oxide is taking place according to [25]:

$$Zn + H_2O \rightarrow ZnO + 2H^+ + 2e^- \quad (9)$$

In the presence of Ni, Ni^{2+} which are formed from the alloy dissolution, are incorporated into the crystal lattice of Cu_2O [26, 27] and the number of cation vacancies decreases with increasing the nickel content [12]. Ni from the alloy segregates into the Cu_2O barrier layer via a solid state reaction and Ni^{2+} interact with mobile cation vacancies which leads to a decrease in the ionic conductivity and an increase of the electronic conductivity of the barrier film and its corrosion resistance thus imcreased [28, 29].

In sulfide containing solutions HS^- will be formed:

$$S^{2-} + H_2O \leftrightarrow HS^- + OH^- \quad (10)$$

HS^- will combine with the metallic copper to form an adsorbed precursor of the oxidation reaction:

$$Cu + HS^- \rightarrow Cu(HS^-)_{ads} \quad (11)$$

The coupled anodic dissolution is then represented by Eq. 12, which is followed by dissociation and recombination processes [30]

$$Cu(HS^-) \rightarrow Cu(HS) + e^- \quad (12)$$

$$Cu(HS) \rightarrow Cu^+ + HS^- \quad (13)$$

$$2Cu^+ + HS^- + OH^- \rightarrow Cu_2S + H_2O \quad (14)$$

and the overall reaction is therefore:

$$4Cu + 2S^{2-} + O_2 + 2H_2O \leftrightarrow 2Cu_2S + 4OH^- \quad (15)$$

However, the presence of Cu_2S prevents dramatically the protective effectiveness of Cu_2O film which is always formed in aqueous solutions, and so the resistance of the passive film decreases in sulfide polluted chloride solutions. Under conditions of low (SH^-) and high Cl^- the formation of the soluble chloride complex, $CuCl_{2-}$, by the reaction with the surface imtermediate, $Cu(SH^-)_{ads}$, could compete with the film formation reaction [18]. Dissolution as $CuCl_{2-}$ via Eq. 16, when SH^- concentration is low at the Cu alloy surface, could lead to the transport of Cu^+ through pores to the Cu_2S/solution interface. At higher SH^- concentration, Cu_2S formation would occur via Eq. 17 and this reaction will dominate at the film/electrolyte interface:

$$Cu(HS^-)_{ads} + 2Cl^- \rightarrow CuCl_{2-} + HS^- + e^- \quad (16)$$

$$2CuCl_{2-} + HS^- \rightarrow 2Cu_2S + 4Cl^- + H^+ \quad (17)$$

Such a transport-deposition process would account for the fine particles, which nucleate and grow on the alloy surfaces at short times.

3.3. Electrochemical impedance spectroscopy, EIS

To confirm the polarization measurements, EIS investigations were carried out. The impedance data of the three different alloys were recorded after 240 h of electrode immersion in the stagnant, naturally aerated neutral 3.5 (m/v) % NaCl solutions containing 2 ppm S^{2-}. Fig. 4 presents these data as Bode plots, since this format enables equal presentation of all impedance data and the appearance of the phase angle as a sensitive parameter for any interfacial phenomena explicitly [31]. In this solution, the Bode plots of the alloys show two phase maxima, the major one at lower frequencies and the other as a shoulder at high frequencies. Such behavior indicates the presence of two time constants representing the electrode processes. The impedance data were analyzed using software provided with the impedance system where the dispersion formula was used. For a simple equivalent circuit model consisting of a parallel combination of a capacitor, C_{dl}, and a resistor, R_{ct}, in series with a resistor, R_s, representing the solution resistance, the electrode impedance, Z, is represented by the mathematical formulation:

$$Z = R_s + [R_{ct} / \{1 + (2\pi f\, R_{ct} C_{dl)\alpha}\}] \quad (18)$$

where $\boldsymbol{\alpha}$ represents an empirical parameter ($\mathbf{0} \leq \boldsymbol{\alpha} \leq 1$) and f is the frequency in Hz [32].

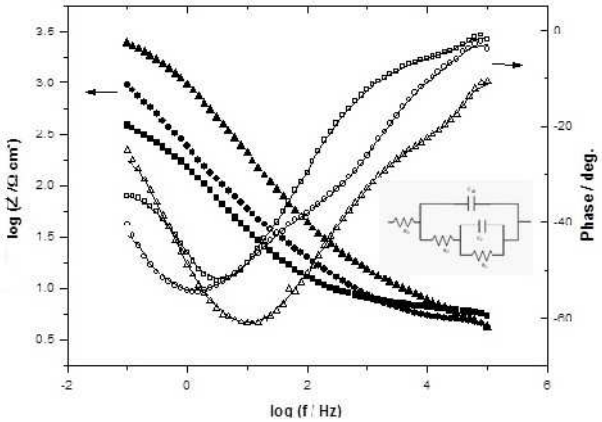

Fig.4: Bode plots of the different alloys after 240 h. immersion in a stagnant naturally aerated neutral 3.5 % NaCl containing 2 ppm S^{2-} solution at 25 ˚C.
Fig.4 (inset): Equivalent circuit model used for impedance data fitting. R_s= solution resistance, R_{ct} = charge-transfer resistance, C_{dl} = double layer capacitance, R_{pf} = passive film resistance, and C_{pf} = passive film capacitance.

To account for the presence of a passive film, the impedance data were analyzed using the equivalent circuit model shown in Fig. 4 (inset), where another combination R_f C_f representing the passive film resistance, R_f, and the porous passive film capacitance, C_f, was introduced. The calculated equivalent circuit parameters for the different alloys are presented in Table 4. The time constant at the intermediate frequencies is originated from the $R_{ct}C_{dl}$ combination while that at low frequencies is due to the R_f C_f combination. The passive film resistance, R_f, of the Cu-10Ni-10Zn alloy is higher than that recorded for the other two alloys, which is in agreement with the polarization experiments. The effect of the immersion time on the stability of the barrier layer, especially on the Cu-10Ni-10Zn alloy surface was investigated. Fig. 5 presents the Bode plots of this alloy in the sulfide polluted chloride solution up to 10 days. The changes in the phase maximum with time indicate the differences in the relaxation time constants at different exposure times. From the corresponding phase angle Bode plots, it can be seen that the angle values at the low frequency zone increase with the immersion time, which indicates a decrease in the corrosion rate of the alloy with time. The same was also recorded with the other two alloys. It is also clear that the total impedance increases with the increase of the immersion time which indicates that the protective film formed on the Cu-10Ni-10Zn alloy becomes more stable with time. The increase of R_f may be explained by the formation of copper sulfide which protects the alloy surface against continuous corrosion. The equivalent circuit parameters for the three different alloys at different time intervals of electrode immersion are presented in Table 4. The data presented in this table show that the barrier film resistance of the Cu-10Ni-10Zn alloy is more than double that of the Cu-10Al-10Zn, which emphasizes its stability. The calculated value of **α** is approximately 1, which means that the barrier layer is behaving like an ideal capacitor [32, 33].

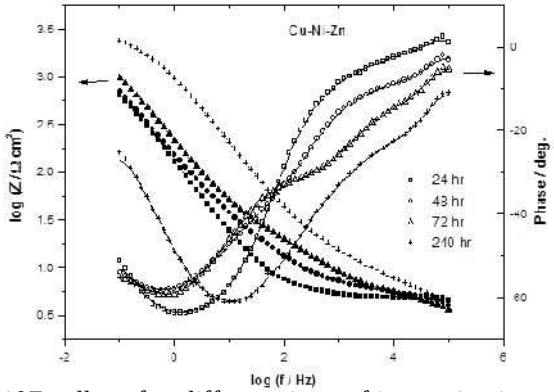

Fig.5: Bode plots of Cu-10Ni-10Zn alloy after different times of immersion in stagnant naturally aerated neutral 3.5 % NaCl containing 2 ppm S^{2-} solution at 25 ◦C.

Table 4: Equivalent circuit parameters for the different Cu-alloys after electrode immersion for different time intervals in stagnant naturally aerated neutral 3.5 % NaCl containing 2 ppm S^{--} at 25 ˚C.

Cu-10Al-10Zn alloy (a

Time /h	**R_s /Ω**	**R_{ct} /Ω cm^2**	**C_{dl} /μF cm^{-2}**	**α_1**	**R_f /kΩ cm^2**	**C_f /μF cm^{-2}**	**α_2**
24	4.1	320	249	1.00	1.6	123	1.00
48	4.1	250	201	0.99	1.9	498	1.00
72	4.2	276	288	0.95	2.1	560	1.00
240	9.1	531	946	0.99	2.0	595	1.00

Cu-10Al-10Ni alloy (b

Time /h	**R_s /Ω**	**R_{ct} /Ω cm^2**	**C_{dl} /μF cm^{-2}**	**α_1**	**R_f /kΩ cm^2**	**C_f /μF cm^{-2}**	**α_2**
24	6.8	600	106	1.00	1.1	1409	1.00
48	3.7	879	52	0.98	1.4	1159	0.99
72	5.2	864	29	0.95	1.8	735	1.00
240	4.6	291	11	0.99	2.4	725	1.00

c) Cu-10Ni-10Zn alloy

Time /h	R_s /Ω	R_{ct} /Ω cm^2	C_{dl} /μF cm^{-2}	α_1	R_f /kΩ cm^2	C_f /μF cm^{-2}	α_2
24	5.1	665	96	1.00	2.1	750	0.99
48	5.2	262	19	1.00	3.1	254	0.99
72	4.2	268	37	0.95	3.9	127	1.00
240	37.9	307	33	0.95	4.2	238	0.99

The electrochemical investigations have shown that the Cu-10Ni-10Zn alloy has the lowest corrosion rate in the sulfide polluted chloride solutions, which can be explained by the anodic reaction of the alloy in this solution. The polarization curves of the different alloys have almost the same shape which means that the electrochemical performance of the three alloys is approximately the same. In this case, the dissolution of Cu represents the rate controlling step. In the Al containing alloys, surface ionization of Al is easier than that of Zn and Ni and a compact alumina layer can be formed, which inhibits the continuous dissolution of copper. In chloride solutions this layer is susceptible to attack and destruction, and so the corrosion rate of the alloy is relatively high [33]. In the presence of Zn and /or Ni the situation is different. The barrier Cu_2O layer is a p-type semiconductor containing cation vacancies as the main defects. NiO is also a p-type semiconductor, whereas ZnO is an n-type semiconductor containing an excess interstitial zinc atoms in the non-stoichiometric compound $Zn_{1+\delta}O$ ($\delta>0$). According to the Solute Vacancy Interaction Model (SVIM), the presence of Ni with copper leads to its segregation in the Cu_2O layer [34]. Also, zinc ions may be incorporated into cation vacancies normally present in the deficient structure of Cu_2O according to:

$$Zn_{Zn}(m) + V_{cu/}(ox) = Zn_{Cu}\bullet(ox) + 2e^- \quad (19)$$

where $Zn_{Zn}(m)$ is a zinc atom in a regular metal site, $V_{cu/}(ox)$ is a negatively charged cation vacancy in the oxide film, and $Zn_{Cu}\bullet(ox)$ is a positively charged Zn cation occupying a metal lattice site. Charged solutes would interact electrostatically with oppositely charged mobile cation vacancies that lead to the formation of a neutral species and thus to a decreased number of cation vacancies.

$$Zn_{Cu}\bullet(ox) + V_{cu/}(ox) = [Zn_{Cu}V_{cu}] \quad (20)$$

It is possible that instead of the incorporation into cation vacancies, zinc ions may simply substitute for Cu^+ ions in the Cu_2O lattice leading to the formation of positively charged incorporated zinc ions. In that case the following one-electron reaction would occur:

$$Cu_{Cu}(ox) + Zn_{Zn}(m) = Zn_{Cu}\bullet(ox) + e^- \quad (21)$$

With increasing nickel content in Cu-xNi alloys, there is a tendency for a greater proportion of Ni^{2+} to replace Cu^+ in Cu_2O [11]. Consequently, the contribution is to a net increase in the ionic resistivity (the annihilation of positive holes is smaller) rather than the incorporation into vacancies, which needs two positive holes to achieve electro-neutrality and this leads to higher corrosion resistance as confirmed by the potentiodynamic polarization experiments and the EIS investigations.

3.4 Surface examinations

The surface morphology of the three alloys was investigated by SEM after 72 h of alloy immersion in sulfide free and sulfide containing chloride solutions. This time was chosen to be sure that the surface

morphology does not subjected to any remarkable change. The results of these investigations for Cu-10Al-10Zn and Cu-10Ni-10Zn alloys are presented in Figs. 6 and 7, respectively.

A B

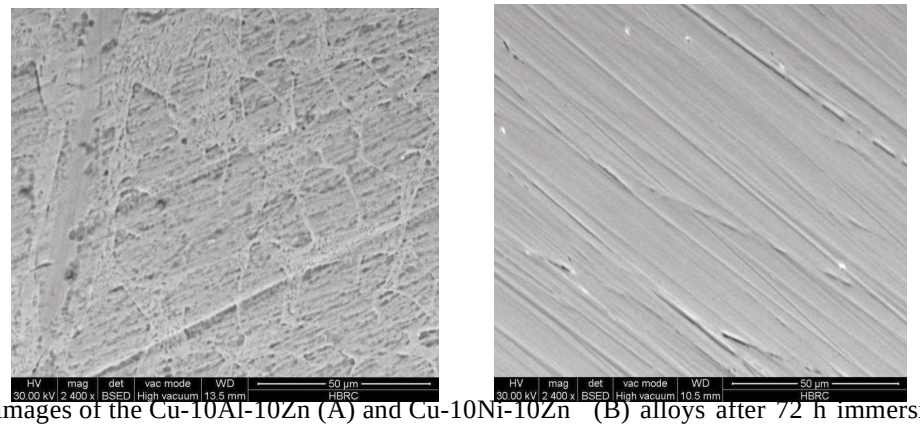

Fig. 6: SEM images of the Cu-10Al-10Zn (A) and Cu-10Ni-10Zn (B) alloys after 72 h immersion in stagnant naturally aerated neutral sulfide free 3.5 % NaCl solution at 25 ˚C.

A B

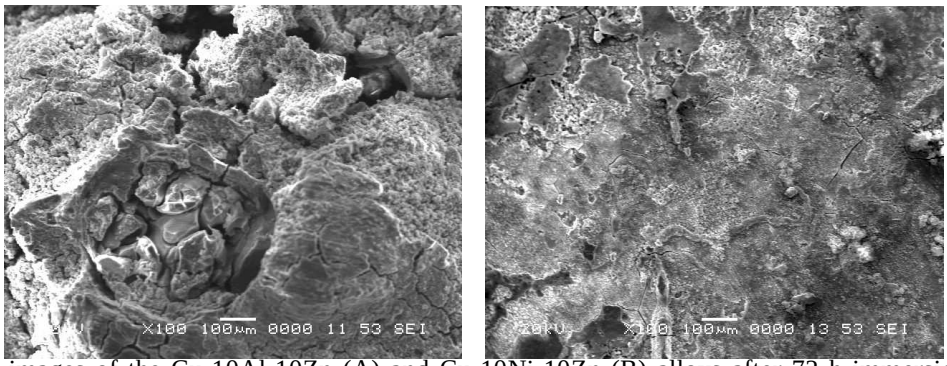

Fig.7: SEM images of the Cu-10Al-10Zn (A) and Cu-10Ni-10Zn (B) alloys after 72 h immersion in stagnant naturally aerated neutral 3.5 % NaCl containing 2 ppm S^{2-} solution at 25 ˚C.

It is clear that the sulfide containing solution is remarkably aggressive as can be seen on the SEM image of Fig. 7. In the sulfide containing solution a granular layer with relatively large sized grains is formed on the alloy surface (cf. Fig. 7 A and B) compared to the smoother surface recorded for sulfide free solutions (cf. Fig. 6 A and B). It is also important to notice that the corrosion products formed on the surface of the different alloys in the chloride solutions containing 2 ppm S^{2-} are relatively more than those formed on the same alloys in absence of sulfide. The surface of Cu-10Al-10Ni alloy after immersion in the test solution was subjected to EDAX analysis as an example and the results of this investigation is presented in Fig. 8, which reveal that the surface film of the alloy is containing sulfide beside Chloride.

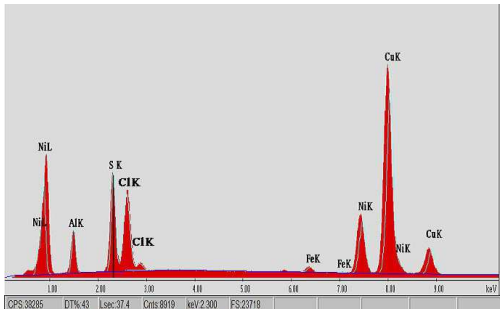

Fig. 8: EDAX analysis of the Cu-10Al-10Ni alloy after immersion in naturally aerated 3.5% NaCl solution containing 2 ppm S^{2-} at 25 ˚C.

These results confirm the polarization and impedance investigations which means that the addition of Ni and Zn to the copper increases the corrosion resistance and hence the stability of the alloy even in sulfide containing chloride solutions increases. Therefore, the Cu-10Ni-10Zn alloy can be recommended as a construction material for sulfide polluted marine environments.

Conclusions

Investigation of the electrochemical behavior of Cu-10Al-10Zn, Cu-10Al-10Ni and Cu-10Ni-10Zn alloys in sulfide polluted chloride solutions have shown that the corrosion rate of the Cu-10Ni-10Zn alloy is less than one fourth of the Cu-10Al-10Zn alloy. The thickness and resistance of the passive film formed on this alloy in the same solution are remarkably larger than those of the passive film formed on the other two alloys. The dissolution of copper is inhibited in the Cu-alloys containing Ni, especially in the presence of Zn. In the presence of Al, the formed Al_2O_3 barrier film is easily destroyed in chloride solutions and the destruction is enhanced by sulfide ions. It is proposed that the incorporation of Ni in the Cu_2O barrier film leads to its stabilization and the stability is enhanced by the presence of Zn. For the industrial applications, it is recommended to use Cu-10Ni-10Zn alloy in sulfide polluted marine environments.

References

[1] Powell CA, Copper-nickel sheathing and its use for ship hulls and off shore structures. Int. Biodeterior. Biodegrad. 1994; 321-31.
[2] Shreir LL, Jarman RA, BursteinGB (Eds). Corrosion: Metal/Environment Reaction. 3rd ed (ButterworthHeinemann Ltd, Linacre House, Jorden Hill, Oxford OX2 8DP, reprinted 1995; p. 4:41, 17:70 and 17:84.
[3] Scully JC. The Fundamentals of Corrosion. Pergamon Press, Oxford, 1990.
[4] Blanco M, Barragan JTC, Barelli N, Noce RD, Fugivara CS, Fernandez J, Benedetti AV. On the electrochemical behavior of Cu-16%Zn-6.5%Al alloy containing the β′-phase (martensite) in borate buffer. Electrochim. Acta 2013; 107: 238- 247.
[5] Chauhan PK, Gadiyar HS. An XPS study of the corrosion of Cu-10 Ni alloy in unpolluted and polluted seawater; the effect of $FeSO_4$ additio., Corros. Sci. 1985; 25:55-68.
[6] Jones DA. Principles and Prevention of Corrosion., 2nd ed., Prentice Hall, Upper Saddle River, NJ, 1996; p. 518.
[7] Kear G, Barker BD, Stokes KR, Walsh FC. Electrochemical Corrosion Behavior of 90-10 Cu-Ni Alloys in Chloride Based Electrolytes. J. Appl. Electrochem. 2004; 34: 659-669.
[8] Schussler A, Exner HE. The corrosion of nickel aluminum bronzes in sea water-I. Protective layer formation and the passivation mechanism. Corros. Sci. 1993; 34: 1793-1802.
[9] Schussler A, Exne HE. The corrosion of nickel-aluminum bronzes in sea water-II. The corrosion mechanism in the presence of sulfide solution. Corros. Sci. 1993; 34: 1803-1811, 34: 1813-1815.
[10] Badawy WA, El-Sherif RM, Shehata H. Electrochemical Behavior of Aluminum Bronze in SulfateChloride Media. J. Appl. Electrochem. 2007; 37: 1099-1106.
[11] North RF, Pryor MJ. The influence of corrosion product structure on the corrosion rate of Cu-Ni alloys. Corros. Sci. 1970; 10: 297-311.
[12] Milosev I, Metikos MH. The behavior of Cu-$_x$Ni (x = 10 to 40 wt %) alloys in alkaline solutions containing chloride ions. Electrochem. Acta 1997; 42: 1537-1548.
[13] Alhaiji JN, Reda MR. On the Effects of Common Pollutants on the Corrosion of Copper-Nickel Alloys in Sulfide Polluted Seawater. J. Electrochem. Soc. 1995; 142: 2944-2953.
[14] Vazquez M, De Sanchez SR. Influence of sulfide ions on the cathodic behavior of copper in 0.1 M borax solution. J. Appl. Electrochem. 1998; 28: 1383-1388.
[15] Jacobs S, Edwards M. Sulfide scale catalysis of copper corrosion. Water Res. 2000; 34: 2798-2808.
[16] Traverso P, Beccaria AM, Poggi G. Effect of sulfides on corrosion of Cu-Ni-Fe-Mn alloy in sea water. Br. Corr. J. 1994; 29: 110-114.
[17] Badawy WA, Al-Kharafi FM, El-Azab AS. Electrochemical Behavior and Corrosion Inhibition of Al, Al6061 and Al-Cu in Neutral Aqueous Solutions, Corros. Sci. 1999; 41: 709-727.
[18] Ostlund HG, Alexander J. Oxidation rate of sulfide in sea water, A preliminary study. J. Geophys. Reas. 1963; 68: 3995-3997.
[19] Benedetti AV, Sumodjo PTA, Nobe K, Cabot PL, Proud WG. Electrochemical studies of copper, copper-aluminium and copper-aluminium-silver alloys: Impedance results in 0.5M NaCl, Electrochim. Acta 1995; 40: 2657-2668.

[20] Badawy WA, Ismail KM, Fathi AM. Effect of Ni content on the corrosion behavior of Cu-Ni alloys in neutral chloride solutions. Electrochim. Acta 2005; 50: 3603-3608.

[21] Zhou XZ, Deng CP, Su YC. Comparative study on the electrochemical performance of the Cu-30Ni and Cu-20Zn-10Ni alloys. J. Alloy and Compounds 2010; 491: 92-97.

[22] Badawy WA, El-Rabiee MM, Hela NH, Nady H. The role of Ni in the surface stability of Cu-Al-Ni ternary alloys in sulfate-chloride solutions. Electrochim. Acta 2012; 71: 50-57.

[23] Kear G, Barker BD, Stokes KR, Walsh FC. Flow influenced electrochemical corrosion of nickel aluminum bronze - Part I. Cathodic polarization, J. Appl. Electrochem. 2004; 34: 1235-1240. And Part II. Anodic polarization and derivation of the mixed potential. 34: 1241-1248.

[24] Chen B, Liang TC, Fu D, Ren D. Corrosion behavior of Cu and the Cu-Zn-Al shape memory alloy in simulated uterine fluid. Contraception 2005; 72: 221-224.

[25] Saber TMH, El-Warraky AA. Electrochemical and spectroscopic studies on dezincification of α brass: Part 1: Effect of pretreatment on surface composition of 70-30 α brass. Br Corros J 1991; 26: 279-285.

[26] Blundy RG, Pryor MJ. The potential dependence of reaction product composition on copper-nickel alloys. Corros. Sci. 1972; 12: 65-75.

[27] Beccaria AM., Crousier J. Dealloying of Cu-Ni alloys in natural sea water. Br. Corr. J. 1989; 24: 49-52.

[28] Urquidi M, Macdonald DD. Solute-Vacancy Interaction Model and the Effect of Minor Alloying Elements on the Initiation of Pitting Corrosion. J. Electrochem. Soc. 1985; 132: 555-562.

[29] Metikoˇs-Hukovi´c M, Babi´c R, Skugor I, Z. Grubaˇc Z. Copper-nickel alloys modified with thin surface films: Corrosion behavior in the presence of chloride ions, Corr. Sci. 2011; 53: 347-352.

[30] Reda MR, Al Hajjaji JN. Deleterious role of complexing agents in corrosion of copper-nickel alloys in sulfide polluted sea water. Br. Corros. J. 1995; 30: 56-62.

[31] Macdonald JR (Ed.). Impedance Spectroscopy. John Wiley & Sons, New York, NY, U.S.A. 1987 (Chapter 4).

[32] Ismail KM, Fathi AM, Badawy WA. Electrochemical behavior of copper-nickel alloys in acidic chloride solutions, Corros. Sci. 2006; 48 1912-1925.

[33] Badawy WA, El-Rabiee MM, Nady H. Synergistic effects of alloying elements in Cu-ternary alloys in chloride solutions. Electrochim. Acta 2014; 120: 39-45.

[34] Macdonald DD, Ben-Haim M, Pallix J. Segregation of alloying elements into passive films. J. Electrochem. Soc. 1989; 136: 3269-3273.